

Few-cycle laser-pulse-assisted electron-atom potential scattering

A. Čerkić¹ and D. B. Milošević^{1,2,3}

¹*Faculty of Science, University of Sarajevo, Zmaja od Bosne 35, 71000 Sarajevo, Bosnia and Herzegovina*

²*Max-Born-Institut, Max-Born-Straße 2a, 12489 Berlin, Germany*

³*Academy of Sciences and Arts of Bosnia and Herzegovina, Bistrik 7, 71000 Sarajevo, Bosnia and Herzegovina*

(Received 6 February 2013; published 21 March 2013)

S-matrix theory of electron-atom scattering assisted by a few-cycle laser pulse is introduced. The result obtained in the first Born approximation corresponds to the direct or single scattering, while the result in the second Born approximation corresponds to the rescattering or double scattering contribution to the laser-assisted scattering process. The rescattered electrons may acquire high energies while moving in the laser pulse. The dependence of the energy spectrum on the value of the carrier-envelope phase and the duration of the laser pulse is investigated. The abrupt cutoffs of the plateau structures in the energy spectra of the process are explained by the classical analysis. It is shown that the height of both the single and double scattering plateaus can be increased by orders of magnitude by choosing the heavier atomic targets.

DOI: [10.1103/PhysRevA.87.033417](https://doi.org/10.1103/PhysRevA.87.033417)

PACS number(s): 34.80.Qb, 34.50.Rk, 33.20.Xx, 03.65.Nk

I. INTRODUCTION

Laser-assisted electron scattering (LAES) is a process in which electrons elastically scatter off atoms or molecules (or their ions) in the presence of a laser field. In this so-called free-free transition n photons are absorbed ($n > 0$) or emitted ($n < 0$) from the laser field so that the initial ($E_i = \mathbf{k}_i^2/2$) and final ($E_f = \mathbf{k}_f^2/2$) electron kinetic energies are connected by the formula $E_f = E_i + n\omega$, where \mathbf{k}_i and \mathbf{k}_f are the corresponding electron momenta and ω is the photon angular frequency (atomic units are used). The LAES was experimentally observed by Weingartshofer *et al.* in 1977 [1]. For a review of later experiments see [2]. From the theoretical side, laser-assisted potential scattering in the first Born approximation (BA) was treated by Bunkin and Fedorov [3], while Kroll and Watson (KW) [4] have obtained the following more general approximate result for the differential cross section (DCS) of LAES with exchange of n photons:

$$\frac{d\sigma_n}{d\Omega}(\mathbf{k}_f, \mathbf{k}_i) = \frac{k_f}{k_i} J_n^2(x) \frac{d\sigma_{el}}{d\Omega}, \quad (1)$$

where J_n is the Bessel function of the first kind of order n and $d\sigma_{el}/d\Omega$ is the field-free elastic DCS. The argument of the Bessel function, $x = \hat{\mathbf{e}}_L \cdot (\mathbf{k}_i - \mathbf{k}_f)I^{1/2}/\omega^2$, is a coupling parameter that depends on the electron energy, laser field intensity I and frequency ω , and the angle between the unit polarization vector $\hat{\mathbf{e}}_L$ of linearly polarized laser field and the momentum change vector of the electron. A review of theoretical results is given in [5].

First experimental results were in good agreement with the KW formula [2] (see also [6], and references therein, for more detailed theoretical and experimental studies). However, in more recent experiments by Wallbank and Holmes [7,8], performed for such scattering geometries that the parameter x is small, the observed DCSs were much larger than the KW prediction. These results have renewed interest for theoretical studies of LAES. However, even with the use of the sophisticated Floquet R -matrix method, it was not possible to explain this discrepancy between the theoretical and experimental results for small values of x (see [9], and references therein). The conclusion was that the most

probable explanation for such experimental results is multiple scattering [10].

In the experiments [1,2,6–8] a pulsed CO₂ laser (wavelength 10.6 μm) with pulse duration $\sim 3 \mu\text{s}$ and the peak intensity up to $4 \times 10^8 \text{ W/cm}^2$ was used, while the targets were argon [1] or other inert atomic gases or molecular gases. The incident electron energies were $< 40 \text{ eV}$. More recently [11], one- and two-photon LAES processes were observed in the experiment with a Nd:YAG laser (wavelength 1.06 μm , pulse duration 6 ns, and the intensity 6 GW/cm^2) and scattering of electrons having the incident energy in the range 50–350 eV off the helium atoms. The results obtained were consistent with the KW formula. Finally, the only experiment in which the LAES was observed using the femtosecond laser was performed by Kanya *et al.* [12]. Since the used pulse duration (200 fs) was only 10^{-7} relative to that used in the experiments [1,2,6–8], only the $n = \pm 1$ photon processes were observed (a slight increase of the DCS for $n = \pm 2$ was also noticed). The wavelength of the used Ti:sapphire laser was 795 nm, while the intensity was $1.8 \times 10^{12} \text{ W/cm}^2$ which is an increase by the factor of 10^3 in comparison with the intensities used in [1,2,6–8]. The 1 keV electrons were scattered off xenon atoms. A successful simulation of this experiment was performed using the result of Ref. [3], according to which the DCS of LAES is given by relation (1) with $d\sigma_{el}/d\Omega$ calculated in the first BA.

In the 1990s a new process in which LAES is important was discovered [13]. This is the so-called high-order above-threshold ionization (HATI), which is described as a three-step process [14]. The first step is above-threshold ionization, a process in which an atom (or molecule) is ionized in such a way that more photons are absorbed from the laser field than is necessary for ionization. The ionized electron, in the second step, moves in the laser field and may return to the parent atomic or molecular core. The returned electron can scatter off this core and, in fact, the third step of HATI is the LAES process, which occurs on an optical-cycle time scale. More recently, it has been suggested to exploit this rescattering process as an ultrafast imaging technique [15], which is called laser-induced electron diffraction (LIED) (see Refs. [16–19] for theoretical and [20–22] for experimental results).

In particular, the HATI by few-cycle pulses has appeared to be very important for the development of a new area of physics—attophysics [23–25]. In order to specify a few-cycle pulse, besides the laser frequency and intensity, one needs additional parameters such as the pulse duration and the carrier-envelope phase (CEP). The CEP is the relative phase between the maximum of the pulse envelope and the nearest maximum of the carrier wave. It determines the shape of a few-cycle pulse and, therefore, the laser-induced or laser-assisted processes in such a pulse. In order to determine the value of CEP various methods were proposed, one of which is the “stereo-HATI” experiment [26–28]. In the context of the above-mentioned LIED, molecular HATI by few-cycle pulses was used in [29] to extract the electron-molecular ion elastic scattering DCSs.

In spite of the importance of HATI by few-cycle pulses, it is interesting that LAES in few-cycle pulses has never been analyzed in detail. This is the aim of the present paper. We will first present the S -matrix theory for scattering in a laser pulse. Next, we will consider LAES within the BA and show that in the second BA an additional plateau appears in the high-energy part of the electron spectrum. As we have mentioned in the first part of the Introduction, it is very difficult to realize the LAES with the femtosecond few-cycle laser pulses. The reason is that, for the Ti:sapphire wavelength of 800 nm, the few-cycle pulses have a duration of only a few femtoseconds, which is too short to achieve an experimental demonstration of LAES. However, very recently, few-cycle strong laser pulses in the mid-infrared region have become available [30–34]. For example, in [34] using a six-cycle pulse having wavelength 3.9 μm , which lasts 80 fs and has the intensity $3.3 \times 10^{14} \text{ W/cm}^2$, it was possible to generate high harmonics of the order 5000. This brings LAES with few-cycle pulses closer to reality. We will present LAES results for such laser pulse parameters. In particular, we will explore the influence of CEP and pulse duration on the scattered electron spectra. Atomic units are used throughout the paper.

II. S-MATRIX THEORY FOR FEW-CYCLE PULSES

The total Hamiltonian of the LAES process is $H(t) = H_0 + V(\mathbf{r}) + V_L(t) = H_V + V_L(t) = H_L(t) + V(\mathbf{r})$, where $H_0 = -\nabla^2/2$, $\nabla \equiv \partial/\partial\mathbf{r}$, $V(\mathbf{r})$ is the scattering potential, and $V_L(t)$ is the interaction with the laser pulse. We introduce the time-evolution operators U , U_L , and U_V of the Hamiltonians $H(t)$, $H_L(t)$, and H_V , respectively. Born expansion (in the scattering potential V) of the total time-evolution operator has the form

$$\begin{aligned} U(t', t) &= U_L(t', t) - i \int_t^{t'} d\tau U_L(t', \tau) V(\mathbf{r}) U_L(\tau, t) \\ &\quad + (-i)^2 \int_t^{t'} d\tau U_L(t', \tau) V(\mathbf{r}) \\ &\quad \times \int_t^\tau d\tau' U_L(\tau, \tau') V(\mathbf{r}) U_L(\tau', t) + \dots \end{aligned} \quad (2)$$

The total time-evolution operator also satisfies the integral equation

$$U(t', t) = U_V(t', t) - i \int_t^{t'} d\tau U(t', \tau) V_L(\tau) U_V(\tau, t). \quad (3)$$

The S -matrix element for transition from the initial to the final plane-wave electron state, governed by the total time-evolution operator $U(t', t)$, is defined by

$$S_{fi} = \lim_{t' \rightarrow \infty} \lim_{t \rightarrow -\infty} e^{i\mathbf{k}_f^2 t'/2} \langle \mathbf{k}_f | U(t', t) | \mathbf{k}_i \rangle e^{-i\mathbf{k}_i^2 t/2}. \quad (4)$$

Let us now be more specific and choose the interaction with the laser pulse in dipole approximation and length gauge. For a linearly polarized (along the z axis) few-cycle laser pulse of duration T_p , with a sine-squared envelope, and with the carrier-envelope phase ϕ , we have $V_L(t) = \mathbf{E}_L(t) \cdot \mathbf{r}$, with

$$\mathbf{E}_L(t) = E_0 \sin^2 \left(\frac{\pi t}{T_p} \right) \cos(\omega t + \phi) \hat{\mathbf{e}}_L, \quad t \in [0, T_p]. \quad (5)$$

Here $E_0 = I^{1/2}$ is the laser field amplitude and we suppose that the pulse length is equal to an integer number n_p of optical cycles $T = 2\pi/\omega$, i.e., $T_p = n_p T$. Since the laser pulse is such that $\mathbf{E}(t) = \mathbf{0}$ for $t \geq T_p$ and for $t \leq 0$, using (3), we obtain

$$U(t', t) = U_V(t', T_p) U(T_p, 0) U_V(0, t). \quad (6)$$

Then Eqs. (4) and (6) imply

$$S_{fi} = \langle \psi_{\mathbf{k}_f}^{(-)}(T_p) | U(T_p, 0) | \psi_{\mathbf{k}_i}^{(+)}(0) \rangle, \quad (7)$$

where $\psi_{\mathbf{k}_f}^{(-)}$ and $\psi_{\mathbf{k}_i}^{(+)}$ are the continuum eigenstates of the Hamiltonian H_V .

Outside the laser field the scattering off the potential V is elastic. Since we are interested in the laser-assisted plateau structures which correspond to absorption or emission of a large number of laser photons we can neglect the scattering after and prior to the laser pulse and approximate the S -matrix element by (up to a phase factor)

$$S_{fi} = \langle \mathbf{k}_f | U(T_p, 0) | \mathbf{k}_i \rangle, \quad (8)$$

where the total time-evolution operator satisfies Eq. (2) with

$$U_L(t', t) = \int d^3\mathbf{k} | \mathbf{k} + \mathbf{A}(t') \rangle \langle \mathbf{k} + \mathbf{A}(t) | e^{(i/2) \int_t^{t'} d\tau [\mathbf{k} + \mathbf{A}(\tau)]^2} \quad (9)$$

and $\mathbf{A}(t) = -\int^t dt' \mathbf{E}(t') = A(t) \hat{\mathbf{e}}_L$. The zeroth-order term in V in Eq. (2) does not contribute and we keep only the first- and second-order terms in V in (2). In this approximation, after a long derivation, which is based on a unification of the method used in Ref. [35] to study LAES by an infinitely long pulse and the strong-field approximation used to study HATI by few-cycle pulses (see Sec. 5.1 of Ref. [24]), the S -matrix element (up to a phase factor) can be written as

$$\begin{aligned} S_{fi} \approx & \int_0^{T_p} dt e^{i(\tilde{E}_f - \tilde{E}_i)t + i(\tilde{\mathbf{k}}_f - \tilde{\mathbf{k}}_i) \cdot \boldsymbol{\alpha}(t)} \left\{ \langle \tilde{\mathbf{k}}_f | V | \tilde{\mathbf{k}}_i \rangle \right. \\ & \left. - i \int_0^t d\tau \left(\frac{2\pi}{i\tau} \right)^{3/2} \langle \tilde{\mathbf{k}}_f | V | \mathbf{k}_s \rangle \langle \mathbf{k}_s | V | \tilde{\mathbf{k}}_i \rangle e^{(i/2)(\mathbf{k}_s - \tilde{\mathbf{k}}_i)^2 \tau} \right\}, \end{aligned} \quad (10)$$

where $\tilde{E}_i = \tilde{\mathbf{k}}_i^2/2$, $\tilde{E}_f = \tilde{\mathbf{k}}_f^2/2$, $\tilde{\mathbf{k}}_i \equiv \mathbf{k}_i - \mathbf{A}(0)$, and $\tilde{\mathbf{k}}_f \equiv \mathbf{k}_f - \mathbf{A}(T_p)$, while the stationary intermediate electron momentum is $\mathbf{k}_s = [\boldsymbol{\alpha}(t - \tau) - \boldsymbol{\alpha}(t)]/\tau$, with $\boldsymbol{\alpha}(t) = \int^t dt' \mathbf{A}(t')$. The shift of the momenta by $\mathbf{A}(0) = \mathbf{A}(T_p) \neq \mathbf{0}$ assures that we calculate the probability of transition from a state with the initial momentum \mathbf{k}_i to a state with the momentum \mathbf{k}_f at the

detector outside the laser field. This is a situation similar to the introduction of the final electron momentum shift in the above-threshold ionization by few-cycle pulses [24].

The first term on the right-hand side of Eq. (10), which is proportional to $\langle \mathbf{k}_f | V | \tilde{\mathbf{k}}_i \rangle = \langle \mathbf{k}_f | V | \mathbf{k}_i \rangle$, describes the process in which the electron, dressed by the few-cycle laser field, scatters once on the potential $V(\mathbf{r})$. The scattering happens at the time t and the integration is over whole pulse duration from $t = 0$ to $t = T_p$. The remaining term in Eq. (10) is the second BA for LAES by a few-cycle pulse. It describes the process in which the electron first scatters off the potential V at the time $t - \tau$, then moves in the laser field during the time from $t - \tau$ to t , and finally rescatters off the potential V at the time t . The integration is over all electron travel times τ from 0 to t and over all rescattering times t from the beginning ($t = 0$) to the end ($t = T_p$) of the pulse. The factor $\tau^{-3/2}$ comes from the saddle-point-method solution of the integral over all intermediate electron momenta \mathbf{k} ($\mathbf{k} \rightarrow \mathbf{k}_s$; see Appendix A in [36]). This second term is responsible for the rescattering plateau in the LAES spectrum which was first found in Ref. [37] (see also [35,38]) for an infinitely long pulse.

For the pulse (5) we have $\alpha(t) = \alpha(t)\hat{\mathbf{e}}_L$, with

$$\alpha(t) = \frac{E_0}{2\omega^2} \left[\cos(\omega t + \phi) - \frac{1}{2} \sum_{j=1,2} \left(\frac{\omega}{\omega_j} \right)^2 \cos(\omega_j t + \phi) \right], \quad (11)$$

and $\omega_1 = \omega + \omega_p$, $\omega_2 = \omega - \omega_p$, $\omega_p = \omega/n_p = 2\pi/T_p$, so that $\alpha(t)$ is time periodic with the period T_p . The exponent with $\alpha(t)$ in (10) can be expanded in a Fourier series $\sum_n c_n \exp(-in\omega_p t)$, where the coefficients c_n can be presented by sums of the generalized Bessel functions [39,40]. In accordance with this, we will calculate only the spectra for the electron energies that satisfy the relation

$$\tilde{E}_f = \tilde{E}_i + n\omega_p, \quad (12)$$

with integer $n > -\tilde{E}_i/\omega_p$. The DCS in the case of potential scattering in a laser pulse can be defined as the differential transition probability per unit time of an electron with the energy $E_f = \mathbf{k}_f^2/2$ into the solid-angle element $d\Omega_{\mathbf{k}_f}$, divided by the flux J_{inc} of incident electron plane wave (along the z axis) $\langle \mathbf{r} | \mathbf{k}_i \rangle = (2\pi)^{-3/2} e^{ik_i z}$, which is $J_{\text{inc}} = k_i/(2\pi)^3$, and multiplied by the energy interval ω_p between the subsequent points determined by (12). The result is

$$\frac{d\sigma_{\tilde{\mathbf{k}}_i}(n)}{d\Omega_{\mathbf{k}_f}} = \frac{|S_{\tilde{\mathbf{k}}_i}|^2}{T_p} \frac{d^3\mathbf{k}_f}{d\Omega_{\mathbf{k}_f} dE_f} \frac{\omega_p}{J_{\text{inc}}} = (2\pi)^3 \omega_p \frac{k_f}{k_i} \frac{|S_{\tilde{\mathbf{k}}_i}|^2}{T_p}. \quad (13)$$

We model the scattering potential by the sum of the polarization potential V_p and the static potential V_s , so that $V = V_p + V_s$. We use the polarization potential

$$V_p(r) = -\frac{\alpha_p}{2(r^2 + d^2)^2}, \quad (14)$$

where α_p is the electrostatic dipole polarizability of the atom that can be found in [41], while the parameter d is connected with α_p and nuclear charge Z by the formula $d^4 = \alpha_p/(2Z^{1/3})$ [42]. Our static potential is modeled by the double Yukawa

potential

$$V_S(r) = -\frac{Z}{H} \frac{e^{-r/D}}{r} [1 + (H-1)e^{-Hr/D}], \quad (15)$$

where $H = DZ^{0.4}$ and the values of D for various atomic targets are given in [43].

III. CLASSICAL ANALYSIS

In order to perform the classical analysis of the single and double scattering, we consider the arguments of the exponential functions in the first and second terms on the right-hand side of Eq. (10). The first term in Eq. (10) describes the direct or single scattering. The argument of the exponential function in the first term is

$$S_D = (\tilde{E}_f - \tilde{E}_i)t + (\tilde{\mathbf{k}}_f - \tilde{\mathbf{k}}_i) \cdot \boldsymbol{\alpha}(t), \quad (16)$$

where t is the scattering time. The stationarity condition $\partial S_D/\partial t = 0$ gives

$$\tilde{\mathbf{k}}_f^2 + 2\mathbf{A}(t) \cdot (\tilde{\mathbf{k}}_f - \tilde{\mathbf{k}}_i) - \tilde{\mathbf{k}}_i^2 = 0, \quad (17)$$

which can be written in the form

$$[\tilde{\mathbf{k}}_i + \mathbf{A}(t)]^2 = [\tilde{\mathbf{k}}_f + \mathbf{A}(t)]^2. \quad (18)$$

This is the electron-energy-conserving condition at the scattering time t . We assume that the initial electron momentum \mathbf{k}_i is in the direction of the laser-field polarization vector $\hat{\mathbf{e}}_L$ and solve Eq. (17) for k_f . The result is

$$(k_f)_{\pm} = -a \cos \theta_f \pm \sqrt{(a \cos \theta_f)^2 + k_i^2 + 2ak_i}, \quad (19)$$

where $a = A(t) - A(T_p)$ and θ_f is the angle between the final electron momentum \mathbf{k}_f and the laser-field polarization vector. This means that the final electron energy $E_f = \mathbf{k}_f^2/2$ can be expressed as a function of the scattering time t .

The second term in Eq. (10) corresponds to the double scattering, i.e., the scattering with a subsequent rescattering. The argument of the exponential function in the second term is

$$S_R = (\tilde{E}_f - \tilde{E}_i)t + (\tilde{\mathbf{k}}_f - \tilde{\mathbf{k}}_i) \cdot \boldsymbol{\alpha}(t) + \frac{\tau}{2}(\mathbf{k}_s - \tilde{\mathbf{k}}_i)^2, \quad (20)$$

where t is the rescattering time and τ is the travel time (i.e., the time between the first scattering and the rescattering). From the conditions $\partial S_R/\partial t = 0$ and $\partial S_R/\partial \tau = 0$ we get

$$\mathbf{k}_s^2 + 2\mathbf{A}(t - \tau) \cdot (\mathbf{k}_s - \tilde{\mathbf{k}}_i) - \tilde{\mathbf{k}}_i^2 = 0, \quad (21)$$

$$\tilde{\mathbf{k}}_f^2 + 2\mathbf{A}(t) \cdot (\tilde{\mathbf{k}}_f - \mathbf{k}_s) - \mathbf{k}_s^2 = 0, \quad (22)$$

which can be rewritten as

$$[\mathbf{k}_s + \mathbf{A}(t - \tau)]^2 = [\tilde{\mathbf{k}}_i + \mathbf{A}(t - \tau)]^2, \quad (23)$$

$$[\tilde{\mathbf{k}}_f + \mathbf{A}(t)]^2 = [\mathbf{k}_s + \mathbf{A}(t)]^2. \quad (24)$$

Equation (23) is the electron-energy-conserving condition at the scattering time $t - \tau$, while Eq. (24) expresses the electron-energy-conserving condition at the rescattering time t . Equations (23) and (24) represent a system of two nonlinear equations which can be solved numerically in order to calculate the final electron energy E_f for different values of the travel time τ . Considering the fact that a large number of travel times may correspond to the same value of energy E_f , we restrict

ourselves to the calculation of the maximum value of E_f and its corresponding travel time τ .

IV. NUMERICAL RESULTS

In all our calculations, we assume that the laser field is linearly polarized with the electric field vector given by Eq. (5) and that the initial electron momentum \mathbf{k}_i is in the direction of the laser-field polarization vector $\hat{\mathbf{e}}_L$.

We first consider the direct scattering of electrons on atomic targets. This process is described by the first term on the right-hand side of Eq. (10). In Fig. 1 the DCS for potential scattering of electrons on He atoms is presented as a function of the final electron energy. The scattering occurs in a linearly polarized few-cycle laser pulse having a wavelength of 3100 nm and an intensity of 4.5×10^{13} W/cm². The carrier-envelope phase of the laser pulse is $\phi = 0^\circ$, while the number of optical cycles n_p is denoted in each panel of Fig. 1. The initial electron energy is $E_i = 15$ eV and the scattering angle of the final-state electrons is $\theta_f = 0^\circ$. The energy spectra in Fig. 1 show a plateau with an abrupt cutoff. The low-energy part of the plateau contains a

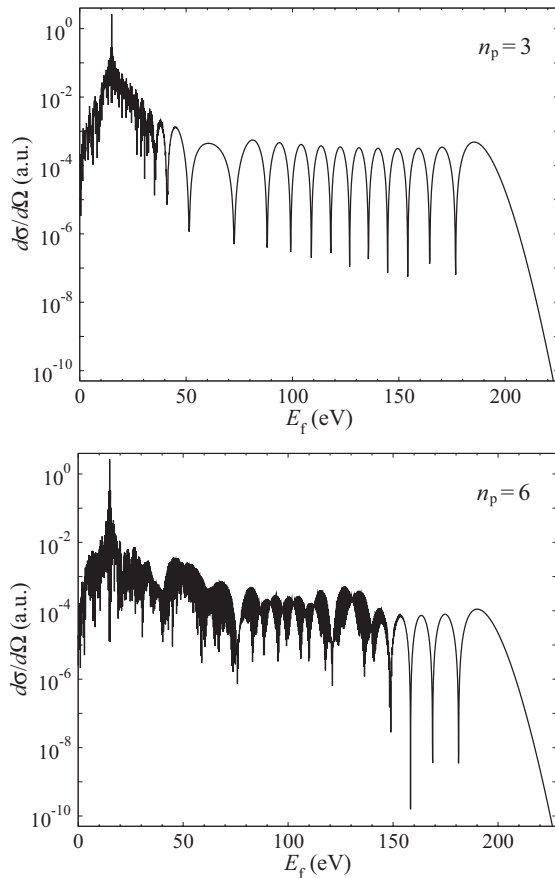


FIG. 1. The DCS for potential scattering of electrons on He atoms in the presence of a linearly polarized few-cycle laser pulse, as a function of the final electron energy E_f . Only the direct (single) scattering is included. The laser pulse has a wavelength of 3100 nm and a peak intensity of 4.5×10^{13} W/cm², while the CEP is $\phi = 0^\circ$. The initial electron energy is $E_i = 15$ eV and the scattering angle of the final-state electrons is $\theta_f = 0^\circ$. The number of optical cycles n_p is denoted in each panel.

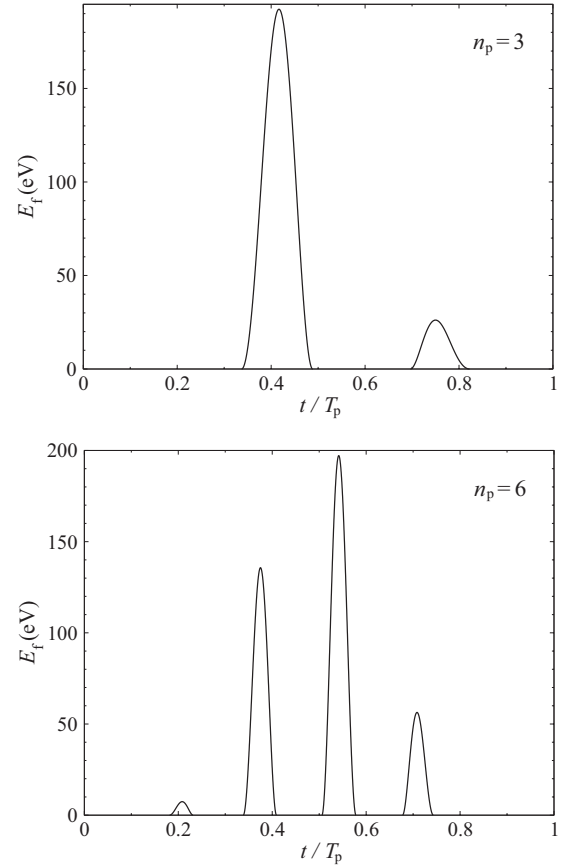


FIG. 2. Classical analysis of the direct scattering solutions for the parameters of Fig. 1. The final electron energy E_f is presented as a function of the scattering time t , expressed in laser-pulse durations T_p . The number of optical cycles n_p is denoted in each panel.

dense oscillatory structure, while the oscillations in the high-energy part of the plateau are much less pronounced. It is also clearly visible that the energy spectrum for six optical cycles is much richer with oscillations than that for three optical cycles. These oscillatory structures and cutoffs of the plateaus in energy spectra can be explained by the classical analysis of the direct scattering. Using Eq. (19) and setting all parameters the same as in Fig. 1, we have calculated the final electron energy E_f as a function of the scattering time t , expressed in units of T_p . The results are presented in Fig. 2, showing that 4 and 8 scattering time solutions exist for $n_p = 3$ and $n_p = 6$, respectively. While all scattering time solutions contribute to the process in the region of very low values of the final electron energy, the number of contributing solutions decreases with an increase of the final electron energy. In the region close to the plateau cutoff just one pair of solutions remains. The highest maximum in each panel of Fig. 2 should match the cutoff energy of the plateau in the corresponding panel of Fig. 1. Comparing Figs. 1 and 2, we conclude that the results obtained by numerical integration of the S matrix [Eqs. (10) and (13)] agree very well with the estimates of the classical analysis [Eq. (19)].

Let us explain the connection between the energy spectra obtained by numerical integration of the S -matrix element and the classical analysis. Instead of numerical integration

over the time t in Eq. (10), the stationary phase method can be used in order to express the S -matrix element as a sum over the stationary points t_s [44]. For a given value of the final electron energy, there is a certain number of stationary points t_s , i.e., the stationary phase solutions. Each of these stationary points gives a contribution to the S -matrix element. These contributions interfere producing the oscillations in the energy spectrum. The interference of more contributions of the stationary points leads to a richer oscillatory structure of the energy spectrum. The stationary points are actually the scattering time solutions t for a given value of the final electron energy E_f , as presented in Fig. 2. For example, let us consider the $n_p = 3$ case shown in the upper panel of Fig. 2. For fixed $E_f < 26$ eV, there are four scattering time solutions (i.e., four stationary points). This means that we have four contributions to the S -matrix element for $E_f < 26$ eV. These contributions interfere producing a dense oscillatory structure in the low-energy part of the spectrum (see the upper panel of Fig. 1). Looking at the upper panel of Fig. 2, one can also notice that there are only two scattering time solutions for $26 \text{ eV} < E_f < 192$ eV, so that only two contributions to the S -matrix element exist. This explains why the oscillations in this part of the energy spectrum are much less pronounced than those observed for $E_f < 26$ eV, as one can see from the upper panel of Fig. 1. For $E_f > 192$ eV, no scattering time solution exists (see the upper panel of Fig. 2) and there is no contribution to the S -matrix element. The plateau in the energy spectrum ends with an abrupt cutoff when E_f increases over 192 eV (see the upper panel of Fig. 1). The connection between the energy spectrum and the scattering time solutions for $n_p = 6$ (the lower panels of Figs. 1 and 2) can be explained using the same arguments. The only difference is that we now have more scattering time solutions, i.e., more contributions to the S -matrix element. This results in a much richer oscillatory structure of the energy spectrum, particularly in the low-energy part of the spectrum. Physically, this oscillatory structure should be understood in terms of Feynman's path integral interpretation of quantum physics [45]. The probability amplitude of the quantum-mechanical scattering process can be represented as a coherent superposition of all possible spatiotemporal paths that connect the initial and the final state of the system [46]. The interference of these contributions is responsible for the mentioned oscillatory structure. For simulation of real experiments the LAES spectra should be averaged over the space-time distribution of laser intensity in focus. Such focal-averaged LAES spectra were calculated in Ref. [47]. In comparison with the fixed intensity spectra, shown in the present paper, the plateaus in the focal-averaged spectra [47] are more inclined and the oscillatory structure is suppressed (or even absent).

We will now analyze electron-atom potential scattering with a subsequent rescattering. In order to include the rescattering effects in our analysis, we take into account both terms on the right-hand side of Eq. (10). We first consider the influence of the CEP ϕ on the energy spectra. The results are shown in Fig. 3, where the DCS for potential scattering of electrons on Ne atoms is presented as a function of the final electron energy. The scattering is assisted by a linearly polarized few-cycle laser pulse having a wavelength of 3100 nm and an intensity of $2.5 \times 10^{13} \text{ W/cm}^2$, while the number of optical cycles is

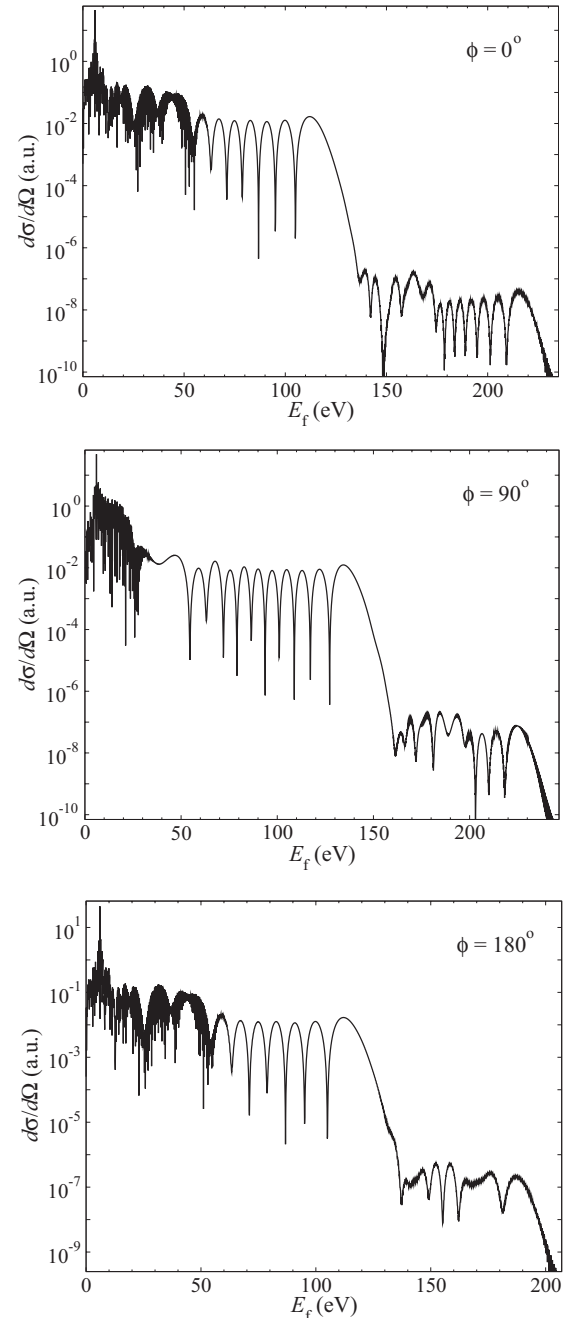


FIG. 3. The DCS for potential scattering of electrons on Ne atoms in the presence of a linearly polarized few-cycle laser pulse, as a function of the final electron energy E_f . Both the direct scattering and rescattering are included. The laser wavelength and peak intensity are 3100 nm and $2.5 \times 10^{13} \text{ W/cm}^2$, respectively, while the number of optical cycles is $n_p = 4$. The initial electron energy is $E_i = 6$ eV and the scattering angle of the final-state electrons is $\theta_f = 0^\circ$. The CEP ϕ is denoted in each panel.

$n_p = 4$. The value of the CEP ϕ is denoted in each panel of Fig. 3. The initial electron energy is $E_i = 6$ eV and the scattering angle of the final-state electrons is $\theta_f = 0^\circ$. There are two plateaus in each panel of Fig. 3. The first plateau is a consequence of the direct scattering of electrons on atomic targets, while the second plateau describes rescattering. One can notice that a change of the CEP affects the oscillatory

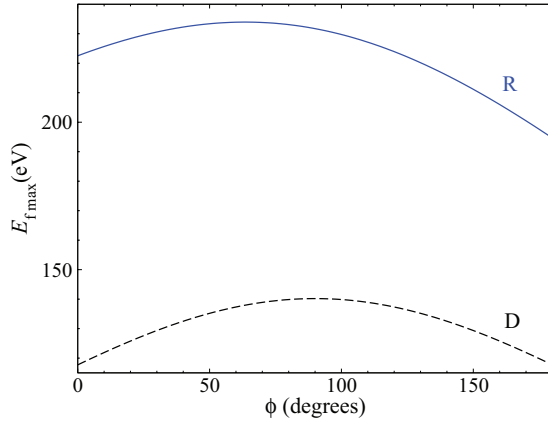


FIG. 4. (Color online) Classical results for the maximum value of the final electron energy in the electron-atom scattering process as a function of the CEP ϕ . The other laser field parameters, the initial electron energy, and the scattering angle are the same as in Fig. 3. The results for direct scattering (dashed black line, denoted by D) and rescattering (solid blue line, denoted by R) are presented.

structure of the energy spectrum and it also shifts the cutoff positions of the plateaus. Using the classical analysis of the direct scattering and rescattering, we can predict how the cutoff energy for the direct scattering and rescattering depends on the CEP. The results are shown in Fig. 4, where the maximum value of the final electron energy is presented as a function of the carrier-envelope phase.

The influence of the scattering angle θ_f on the plateau structures in energy spectra is analyzed in Fig. 5, where the DCS for potential scattering of electrons on He atoms is presented as a function of the final electron energy. The wavelength and peak intensity of the few-cycle laser pulse are 3300 nm and 3×10^{13} W/cm², respectively. The CEP of the pulse is $\phi = 0^\circ$ and the number of optical cycles is $n_p = 4$. The initial electron energy is $E_i = 10$ eV and the scattering angle θ_f is denoted in each panel of Fig. 5. The results presented in Fig. 5 clearly show that the plateau structures in energy spectra are strongly dependent on the scattering angle of the final-state electrons. If the scattering angle is increased from $\theta_f = 0^\circ$ to a certain value, the cutoff energy of both plateaus decreases and the plateaus become shorter. A further increase of the scattering angle causes an increase of the cutoff energy and the plateaus become longer. For large values of the scattering angle ($\theta_f > 90^\circ$), the first plateau is longer than the second one, so that the rescattering effects are masked by the direct scattering contribution. This behavior of the plateaus in the energy spectrum is confirmed by our classical analysis. The results of the classical analysis are illustrated in Fig. 6, where the maximum value of the final electron energy is presented as a function of the scattering angle θ_f .

We will now consider how the number of optical cycles of the laser pulse affects the energy spectrum of electron-atom scattering when rescattering effects are included. In Fig. 7 the DCS for potential scattering of electrons on Ar atoms is presented as a function of the final electron energy. The wavelength and peak intensity of the few-cycle laser pulse are 3000 nm and 1.8×10^{13} W/cm², respectively. The CEP of the pulse is $\phi = 0^\circ$, while the number of optical cycles

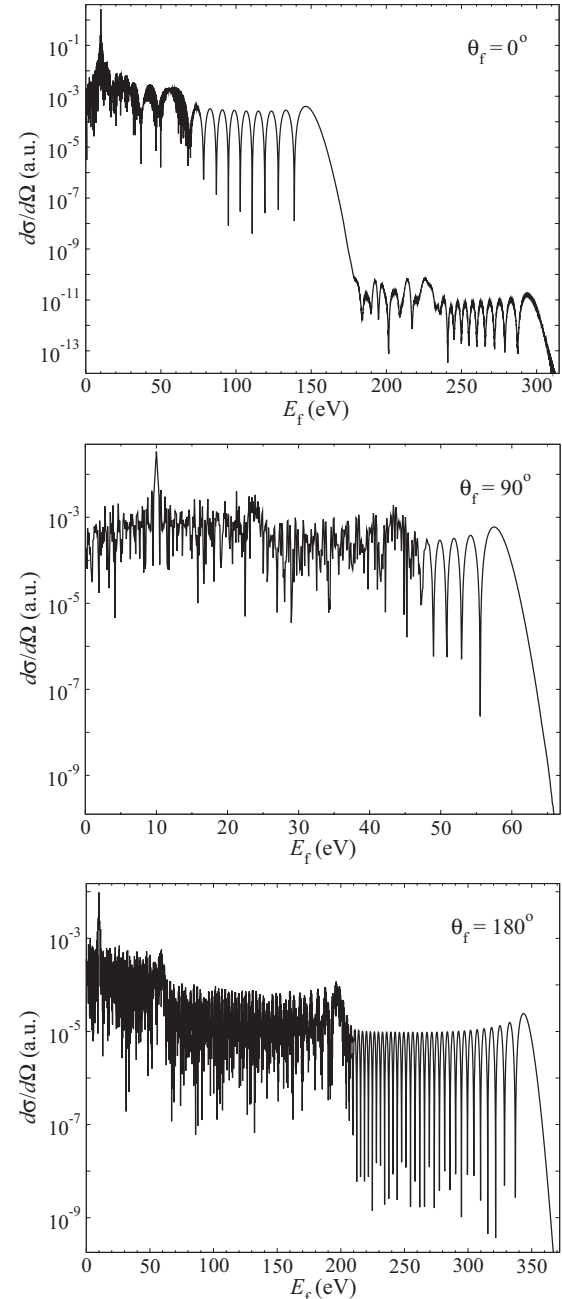


FIG. 5. The DCS for potential scattering of electrons on He atoms in the presence of a linearly polarized few-cycle laser pulse, as a function of the final electron energy E_f . Both the direct scattering and rescattering are included. The laser pulse has a wavelength of 3300 nm and a peak intensity of 3×10^{13} W/cm². The CEP of the pulse is $\phi = 0^\circ$ and the number of optical cycles is $n_p = 4$. The initial electron energy is $E_i = 10$ eV, while the scattering angle θ_f is denoted in each panel.

n_p is denoted in each panel of Fig. 7. The initial electron energy is $E_i = 5$ eV and the scattering angle of the final-state electrons is $\theta_f = 0^\circ$. When we have previously considered the direct scattering, we have seen that the oscillations in the energy spectrum were denser and more pronounced for a larger number of optical cycles (the energy spectra for $n_p = 3$ and $n_p = 6$ were compared). The same is true for the rescattering,

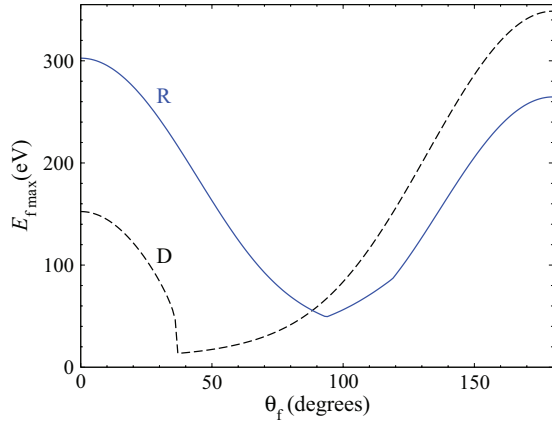


FIG. 6. (Color online) Classical results for the maximum value of the final electron energy in the electron-atom scattering process as a function of the scattering angle θ_f . The laser field parameters and the initial electron energy are the same as in Fig. 5. The results for direct scattering (dashed black line, denoted by D) and rescattering (solid blue line, denoted by R) are presented.

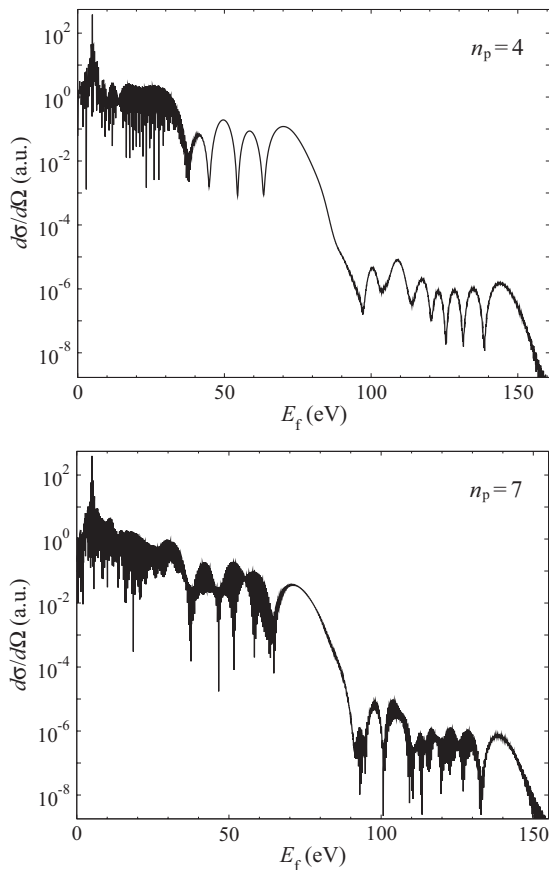


FIG. 7. The DCS for potential scattering of electrons on Ar atoms in the presence of a linearly polarized few-cycle laser pulse, as a function of the final electron energy E_f . Both the direct scattering and rescattering are included. The laser wavelength and peak intensity are 3000 nm and 1.8×10^{13} W/cm², respectively, while the CEP is $\phi = 0^\circ$. The initial electron energy is $E_i = 5$ eV and the scattering angle of the final-state electrons is $\theta_f = 0^\circ$. The number of optical cycles n_p is denoted in each panel.

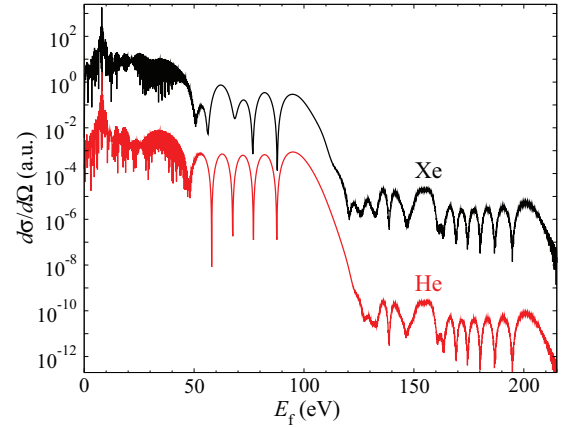


FIG. 8. (Color online) The DCS for potential scattering of electrons in the presence of a linearly polarized few-cycle laser pulse, as a function of the final electron energy E_f . Both the direct scattering and rescattering are included. The laser pulse has a wavelength of 3000 nm and a peak intensity of 2.5×10^{13} W/cm². The CEP of the pulse is $\phi = 0^\circ$ and the number of optical cycles is $n_p = 4$. The initial electron energy is $E_i = 8$ eV, while the scattering angle is $\theta_f = 0^\circ$. The results for scattering of electrons on Xe (upper black line, denoted by Xe) and He atoms (lower red line, denoted by He) are presented.

as we can see from Fig. 7 where the energy spectra for $n_p = 4$ and $n_p = 7$ are presented. Figure 7 shows that both the direct-scattering and the rescattering plateau show a richer oscillatory structure for a larger number of optical cycles, i.e., for $n_p = 7$. This can be explained by the fact that the number of classical solutions for scattering and rescattering times increases with the increase of n_p . We have already illustrated this fact for direct scattering (see Fig. 2).

The choice of the atomic target does not affect the maximum value of the final electron energy for the direct scattering and rescattering, but it does affect the value of the DCS. This is illustrated in Fig. 8, where the DCSs for potential scattering of electrons on He and Xe atoms are presented as functions of the final electron energy. The wavelength and peak intensity of the few-cycle laser pulse are 3000 nm and 2.5×10^{13} W/cm², respectively. The CEP of the pulse is $\phi = 0^\circ$, while the number of optical cycles is $n_p = 4$. The initial electron energy is $E_i = 8$ eV and the scattering angle of the final-state electrons is $\theta_f = 0^\circ$. Figure 8 shows that, while the cutoff positions of the direct-scattering and rescattering plateau are the same for He and Xe, the DCS for electron scattering on Xe atoms is much larger than that for electron scattering on He atoms. The difference is three orders of magnitude for direct scattering (first plateau) and five orders of magnitude for rescattering (second plateau). This leads to the conclusion that the process can be enhanced by the use of heavier atomic targets.

V. CONCLUSIONS

In spite of the fact that the LAES was one of the first observed multiphoton processes it still attracts the attention of both theoretical and experimental physicists. The LAES process is a part (the third step) of the HATI process

and is characterized by the femtosecond time scale. Recent experimental findings [30–34] have stimulated us to explore the LAES process using few-cycle mid-infrared laser pulses.

We have formulated the S -matrix theory of few-cycle laser-pulse-assisted electron-atom potential scattering. As in the case of an infinitely long flat pulse, in the few-cycle pulse case both the direct and rescattering plateaus develop in the LAES spectra. We have shown that the length of these plateaus depends on the value of CEP so that the cutoff position can be controlled changing the CEP, and vice versa, the measurement of the cutoff position can be used for determining the value of CEP.

We have also explored the dependence of the structure of LAES spectra on the laser pulse duration and found that

for longer pulses the spectrum is characterized by regions of wild oscillations. Using our classical analysis we have shown that the reason for such oscillations is the interference of a large number of quantum orbits [24,44,45]. For shorter pulses (consisting of three to four optical cycles) the number of such (classical) solutions is smaller and wild oscillations appear only for low energies of the final electrons.

ACKNOWLEDGMENTS

Sponsorship has been provided by the Alexander von Humboldt Foundation and funding by the German Federal Ministry of Education and Research in the framework of the Research Group Linkage Programme.

-
- [1] A. Weingartshofer, J. K. Holmes, G. Caudle, E. M. Clarke, and H. Kruger, *Phys. Rev. Lett.* **39**, 269 (1977).
- [2] N. J. Mason, *Rep. Prog. Phys.* **56**, 1275 (1993).
- [3] F. V. Bunkin and M. V. Fedorov, *Zh. Eksp. Teor. Phys.* **49**, 1215 (1965) [*Sov. Phys. JETP* **22**, 844 (1965)].
- [4] N. M. Kroll and K. M. Watson, *Phys. Rev. A* **8**, 804 (1973).
- [5] F. Ehlötzky, A. Jaroń, and J. Z. Kamiński, *Phys. Rep.* **297**, 63 (1998).
- [6] D. Nehari, J. Holmes, K. M. Dunseath, and M. Terao-Dunseath, *J. Phys. B* **43**, 025203 (2010).
- [7] B. Wallbank and J. K. Holmes, *Phys. Rev. A* **48**, R2515 (1993); *J. Phys. B* **27**, 1221 (1994); **27**, 5405 (1994); *Can. J. Phys.* **79**, 1237 (2001).
- [8] M. O. Musa, A. MacDonald, L. Tidswell, J. Holmes, and B. Wallbank, *J. Phys. B* **43**, 175201 (2010).
- [9] N. Morrison and C. H. Greene, *Phys. Rev. A* **86**, 053422 (2012).
- [10] I. Rabadán, L. Méndez, and A. S. Dickinson, *J. Phys. B* **29**, L801 (1996); D. B. Milošević and F. Ehlötzky, *ibid.* **30**, 2999 (1997).
- [11] B. A. deHarak, L. Ladino, K. B. MacAdam, and N. L. S. Martin, *Phys. Rev. A* **83**, 022706 (2011).
- [12] R. Kanya, Y. Morimoto, and K. Yamanouchi, *Phys. Rev. Lett.* **105**, 123202 (2010); *Rev. Sci. Instrum.* **82**, 123105 (2011).
- [13] B. Yang, K. J. Schafer, B. Walker, K. C. Kulander, P. Agostini, and L. F. DiMauro, *Phys. Rev. Lett.* **71**, 3770 (1993); G. G. Paulus, W. Nicklich, H. Xu, P. Lambropoulos, and H. Walther, *ibid.* **72**, 2851 (1994).
- [14] P. B. Corkum, *Phys. Rev. Lett.* **71**, 1994 (1993); K. J. Schafer, B. Yang, L. F. DiMauro, and K. C. Kulander, *ibid.* **70**, 1599 (1993).
- [15] T. Zuo, A. D. Bandrauk, and P. B. Corkum, *Chem. Phys. Lett.* **259**, 313 (1996).
- [16] M. Spanner, O. Smirnova, P. B. Corkum, and M. Yu. Ivanov, *J. Phys. B* **37**, L243 (2004); S. N. Yurchenko, S. Patchkovskii, I. V. Litvinyuk, P. B. Corkum, and G. L. Yudin, *Phys. Rev. Lett.* **93**, 223003 (2004).
- [17] T. Morishita, A.-T. Le, Z. Chen, and C. D. Lin, *Phys. Rev. Lett.* **100**, 013903 (2008); Z. Chen, A. T. Le, T. Morishita, and C. D. Lin, *Phys. Rev. A* **79**, 033409 (2009).
- [18] M. V. Frolov, N. L. Manakov, and A. F. Starace, *Phys. Rev. A* **79**, 033406 (2009).
- [19] A. Čerkić, E. Hasović, D. B. Milošević, and W. Becker, *Phys. Rev. A* **79**, 033413 (2009).
- [20] M. Okunishi, T. Morishita, G. Prümper, K. Shimada, C. D. Lin, S. Watanabe, and K. Ueda, *Phys. Rev. Lett.* **100**, 143001 (2008); D. Ray, B. Ulrich, I. Bocharova, C. Maharjan, P. Ranitovic, B. Gramkow, M. Magrakvelidze, S. De, I. V. Litvinyuk, A. T. Le, T. Morishita, C. D. Lin, G. G. Paulus, and C. L. Cocke, *ibid.* **100**, 143002 (2008).
- [21] M. Meckel, D. Comtois, D. Zeidler, A. Staudte, D. Pavičić, H. C. Bandulet, H. Pépin, J. C. Kieffer, R. Dörner, D. M. Villeneuve, and P. B. Corkum, *Science* **320**, 1478 (2008).
- [22] C. Cornaggia, *Phys. Rev. A* **78**, 041401(R) (2008); *J. Phys. B* **42**, 161002 (2009); *Phys. Rev. A* **82**, 053410 (2010).
- [23] T. Brabec and F. Krausz, *Rev. Mod. Phys.* **72**, 545 (2000).
- [24] D. B. Milošević, G. G. Paulus, D. Bauer, and W. Becker, *J. Phys. B* **39**, R203 (2006).
- [25] F. Krausz and M. Ivanov, *Rev. Mod. Phys.* **81**, 163 (2009).
- [26] G. G. Paulus, F. Lindner, H. Walther, A. Baltuška, E. Goulielmakis, M. Lezius, and F. Krausz, *Phys. Rev. Lett.* **91**, 253004 (2003).
- [27] D. B. Milošević, G. G. Paulus, and W. Becker, *Opt. Express* **11**, 1418 (2003); *Laser Phys. Lett.* **1**, 93 (2004).
- [28] T. Rathje, N. G. Johnson, M. Möller, F. Süßmann, D. Adolph, M. Kübel, R. Kienberger, M. F. Kling, G. G. Paulus, and A. M. Saylor, *J. Phys. B* **45**, 074003 (2012).
- [29] A. Gazibegović-Busuladžić, E. Hasović, M. Busuladžić, D. B. Milošević, F. Kelkensberg, W. K. Siu, M. J. J. Vrakking, F. Lépine, G. Sansone, M. Nisoli, I. Znakovskaya, and M. F. Kling, *Phys. Rev. A* **84**, 043426 (2011).
- [30] O. D. Mücke, S. Ališauskas, A. J. Verhoef, A. Pugžlys, A. Baltuška, V. Smilgevičius, J. Pocius, L. Giniūnas, R. Danielius, and N. Forget, in *Advances in Solid-State Lasers: Development and Applications*, edited by M. Grishin (InTech, Croatia, 2010), p. 279.
- [31] A. D. DiChiara, E. Sistrunk, C. I. Blaga, U. B. Szafruga, P. Agostini, and L. F. DiMauro, *Phys. Rev. Lett.* **108**, 033002 (2012).
- [32] C. I. Blaga, J. Xu, A. D. DiChiara, E. Sistrunk, K. Zhang, P. Agostini, T. A. Miller, L. F. DiMauro, and C. D. Lin, *Nature (London)* **483**, 194 (2012).

- [33] J. Xu, C. I. Blaga, A. D. DiChiara, E. Sistrunk, K. Zhang, Z. Chen, A.-T. Le, T. Morishita, C. D. Lin, P. Agostini, and L. F. DiMauro, *Phys. Rev. Lett.* **109**, 233002 (2012).
- [34] T. Popmintchev, M.-C. Chen, D. Popmintchev, P. Arpin, S. Brown, S. Ališauskas, G. Andriukaitis, T. Balčiunas, O. D. Mücke, A. Pugzlys, A. Baltuška, B. Shim, S. E. Schrauth, A. Gaeta, C. Hernández-García, L. Plaja, A. Becker, A. Jaron-Becker, M. M. Murnane, and H. C. Kapteyn, *Science* **336**, 1287 (2012).
- [35] A. Čerkić and D. B. Milošević, *Phys. Rev. A* **70**, 053402 (2004); *Laser Phys.* **15**, 268 (2005).
- [36] A. Gazibegović-Busuladžić, D. B. Milošević, and W. Becker, *Phys. Rev. A* **70**, 053403 (2004).
- [37] N. L. Manakov, A. F. Starace, A. V. Flegel, and M. V. Frolov, *Pis'ma Zh. Eksp. Teor. Fiz.* **76**, 316 (2002) [*JETP Lett.* **76**, 258 (2002)].
- [38] A. V. Flegel, M. V. Frolov, N. L. Manakov, and A. N. Zheltukhin, *J. Phys. B* **42**, 241002 (2009).
- [39] D. B. Milošević, *J. Phys. B* **29**, 875 (1996).
- [40] J. Zhang, X. Feng, Z. Xu, and D.-S. Guo, *Phys. Rev. A* **69**, 043409 (2004).
- [41] A. A. Radzig and B. M. Smirnov, *Reference Data on Atoms, Molecules and Ions* (Springer, Berlin, 1985).
- [42] M. H. Mittleman and K. M. Watson, *Phys. Rev.* **113**, 198 (1959).
- [43] A. E. S. Green, D. L. Sellin, and A. S. Zachor, *Phys. Rev.* **184**, 1 (1969).
- [44] A. Čerkić and D. B. Milošević, *Phys. Rev. A* **73**, 033413 (2006).
- [45] P. Salières, B. Carré, L. Le Déroff, F. Grasbon, G. G. Paulus, H. Walther, R. Kopold, W. Becker, D. B. Milošević, A. Sanpera, and M. Lewenstein, *Science* **292**, 902 (2001).
- [46] D. B. Milošević, D. Bauer, and W. Becker, *J. Mod. Opt.* **53**, 125 (2006).
- [47] A. Čerkić and D. B. Milošević, *Phys. Rev. A* **75**, 013412 (2007).